

The Effect of Memory and Active Forces on Transition Path Time Distributions

Peer-reviewed author version

Carlon, Enrico; Orland, Hubert; Sakaue, Takahiro & VANDERZANDE, Carlo (2018)

The Effect of Memory and Active Forces on Transition Path Time Distributions. In:

JOURNAL OF PHYSICAL CHEMISTRY B, 122 (49), p. 11186-11194.

DOI: 10.1021/acs.jpcb.8b06379

Handle: <http://hdl.handle.net/1942/27754>

The Effect of Memory and Active Forces on Transition Path Time Distributions

Enrico Carlon, Henri Orland, Takahiro Sakaue, and Carlo Vanderzande

J. Phys. Chem. B, **Just Accepted Manuscript** • DOI: 10.1021/acs.jpcb.8b06379 • Publication Date (Web): 13 Aug 2018

Downloaded from <http://pubs.acs.org> on August 21, 2018

Just Accepted

“Just Accepted” manuscripts have been peer-reviewed and accepted for publication. They are posted online prior to technical editing, formatting for publication and author proofing. The American Chemical Society provides “Just Accepted” as a service to the research community to expedite the dissemination of scientific material as soon as possible after acceptance. “Just Accepted” manuscripts appear in full in PDF format accompanied by an HTML abstract. “Just Accepted” manuscripts have been fully peer reviewed, but should not be considered the official version of record. They are citable by the Digital Object Identifier (DOI®). “Just Accepted” is an optional service offered to authors. Therefore, the “Just Accepted” Web site may not include all articles that will be published in the journal. After a manuscript is technically edited and formatted, it will be removed from the “Just Accepted” Web site and published as an ASAP article. Note that technical editing may introduce minor changes to the manuscript text and/or graphics which could affect content, and all legal disclaimers and ethical guidelines that apply to the journal pertain. ACS cannot be held responsible for errors or consequences arising from the use of information contained in these “Just Accepted” manuscripts.



The Effect of Memory and Active Forces on Transition Path Time Distributions

E. Carlon,^{*,†} H. Orland,^{*,‡,¶} T. Sakaue,^{*,§,||} and C. Vanderzande^{*,⊥,†}

*KU Leuven, Institute for Theoretical Physics, Celestijnenlaan 200D, 3001 Leuven, Belgium,
Institut de Physique Théorique, CEA, CNRS, UMR3681, F-91191 Gif-sur-Yvette, France,
Beijing Computational Science Research Center, No.10 East Xibeiwang Road, Beijing
100193, China, Department of Physics and Mathematics, Aoyama Gakuin University,
5-10-1 Fuchinobe, Chuo-ku, Sagamihara, Kanagawa 252-5258, Japan, PRESTO, Japan
Science and Technology Agency (JST), 4-1-8 Honcho Kawaguchi, Saitama 332-0012,
Japan, and Faculty of Sciences, Hasselt University, 3590 Diepenbeek, Belgium*

E-mail: enrico.carlon@kuleuven.be; henri.orland@cea.fr; sakaue@phys.aoyama.ac.jp;
carlo.vanderzande@uhasselt.be

Abstract

An analytical expression is derived for the transition path time distribution for a one-dimensional particle crossing of a parabolic barrier. Two cases are analyzed: (i) A non-Markovian process described by a generalized Langevin equation with a power-law memory kernel and (ii) a Markovian process with a noise violating the fluctuation-dissipation theorem, modeling the stochastic dynamics generated by active forces. In the case (i) we show that the anomalous dynamics strongly affecting the short time behavior of the distributions, but this happens only for very rare events not influ-

encing the overall statistics. At long times the decay is always exponential, in disagreement with a recent study suggesting a stretched exponential decay. In the case (ii) the active forces do not substantially modify the short time behavior of the distribution, but lead to an overall decrease of the average transition path time. These findings offer some novel insights, useful for the analysis of experiments of transition path times in (bio)molecular systems.

Introduction

Biomolecular folding involves structural transitions of various time- and lengthscales. A simplified description of this process employs a single reaction coordinate performing stochastic dynamics along a free energy landscape. In the case of a two state folding, the folded and unfolded states correspond to two free energy minima, which are separated by a barrier. Typically, this barrier is high compared to the characteristic thermal energy $k_B T$, therefore the molecule spends the predominant fraction of its time close to one of the minima.¹ Transition paths are the part of the stochastic trajectory corresponding to an actual barrier crossing event.² Although the transition paths cor-

^{*}To whom correspondence should be addressed

[†]KU Leuven, Institute for Theoretical Physics, Celestijnenlaan 200D, 3001 Leuven, Belgium

[‡]Institut de Physique Théorique, CEA, CNRS, UMR3681, F-91191 Gif-sur-Yvette, France

[¶]Beijing Computational Science Research Center, No.10 East Xibeiwang Road, Beijing 100193, China

[§]Department of Physics and Mathematics, Aoyama Gakuin University, 5-10-1 Fuchinobe, Chuo-ku, Sagamihara, Kanagawa 252-5258, Japan

^{||}PRESTO, Japan Science and Technology Agency (JST), 4-1-8 Honcho Kawaguchi, Saitama 332-0012, Japan

[⊥]Faculty of Sciences, Hasselt University, 3590 Diepenbeek, Belgium

respond to a tiny fraction of the stochastic trajectory, they encompass all the information of the folding process. Measuring their duration has been for long time a big challenge, owing to the high time resolution needed. In the past few years, however, experiments have sufficiently progressed to make measurements of transition path times in nucleic acids and protein folding possible.³⁻⁶ Recently also the full probability distribution function of transition path times, obtained from the statistics of a large number of events, was determined.⁷ The theory of transition path times have been discussed in several papers.⁸⁻¹⁸ These studies mostly employed memoryless Markovian dynamics, while correlated noise, leading to memory effects and anomalous dynamics, was only considered in a few recent works.^{19,20}

Anomalous dynamics is ubiquitous in macromolecular systems as polymers, as it is known from many examples.²¹⁻²⁷ This dynamics is characterized by a mean-square displacement of a suitable reaction coordinate scaling as $\langle \Delta x^2 \rangle \sim t^\alpha$, with $\alpha \neq 1$. The analysis of the effect of an underlying anomalous dynamics on transition path times is therefore an interesting case to study, which is one of the aims of this paper. Another purpose of the present work is to analyze transition path times for stochastic processes in which the noise has a non-thermal component, ie not satisfying a fluctuation-dissipation relation. Such noise has been used in the description of the dynamics of active systems.²⁸ Our primary interest is to calculate the transition path time (TPT) distribution for these two cases and discuss the differences with the more standard situation of Markovian dynamics in thermal systems. We consider here a parabolic barrier, which leads to a dynamics described by linear stochastic differential equations and to Gaussian processes. We show that, using the formalism developed recently in Ref.,¹⁸ the calculations are manageable and lead to some simple expressions for the TPT distributions. We discuss here several features of these distributions such as the short and long time behavior in the limit of high barriers.

Generalities

We consider a particle performing a stochastic dynamics on an inverted parabolic potential barrier $V(x) = -kx^2/2$, with $k > 0$. At time $t = 0$ the particle starts from a point $-x_0 + \varepsilon$. Transition paths are those paths reaching x_0 at the right side of the barrier without recrossing $-x_0$ and x_0 . To compute the distribution of their duration one should solve the Langevin equation imposing absorbing boundary conditions in $-x_0$ and x_0 . Free boundary conditions are however easier to handle and provide a good approximation if the barrier is high,¹⁰ i.e. $\beta E \gg 1$, with $E = kx_0^2/2$ and $\beta = 1/k_B T$ the inverse temperature. This is because the probability of multiple crossings in $\pm x_0$ is negligible for high barriers. **The absorbing boundaries TPT distribution can be expressed as an infinite sum of hypergeometric functions, which has to be evaluated numerically.²⁹ Typically, absorbing boundaries give rise to shorter average TPT compared to the free boundaries.^{10,29} For a systematic comparison between the two boundary conditions see.²⁹ Here we focus on the free boundary case for which, as we shall show, a simple exact analytical solution is available.**

In Ref.¹⁸ the **free boundary condition** TPT distribution was calculated for a Markovian particle with inertia. It was shown that both in the inertial and overdamped cases the TPT distribution assumes the general form¹⁸

$$p_{TP}(t) = -\frac{2}{\sqrt{\pi}} \frac{\dot{G}(t)e^{-G^2(t)}}{1 - \text{Erf}(\sqrt{\beta E})}. \quad (1)$$

where $\dot{G} \equiv dG/dt$ and

$$G(t) \equiv \frac{x_0 - \bar{x}(t)}{\sqrt{2\sigma^2(t)}}. \quad (2)$$

In the previous equation

$$\bar{x}(t) \equiv \langle x(t) \rangle \quad (3)$$

$$\sigma^2(t) \equiv \langle (x(t) - \bar{x}(t))^2 \rangle \quad (4)$$

are the mean and variance of the process.

In the overdamped case the function $G(t)$ as-

sumes a simple form

$$G(t) = \sqrt{\beta E} \sqrt{\frac{e^{\Omega t} + 1}{e^{\Omega t} - 1}} \quad (5)$$

where $\Omega = k/\gamma$ and γ is the friction coefficient. The $G(t)$ in the inertial case is more complex and is given in Ref.¹⁸

For short times $G(t) \approx \sqrt{2}x_0/\sigma(t)$, which diverges as a consequence of the the initial condition $x(0) = -x_0$, implying $\sigma(t) \rightarrow 0$. This leads to a TPT distribution vanishing with an essential singularity as $t \rightarrow 0$. In the Markovian case the behavior was found to be different in the overdamped $p_{\text{TP}}(t) \sim \exp(-x_0^2/Dt)$ and inertial $p_{\text{TP}}(t) \sim \exp(-2\beta m x_0^2/t^2)$ cases¹⁸ (here m is the particle mass and $D = 1/(\beta\gamma)$ the diffusion coefficient). At long times $G(t)$ converges to a constant in both cases, while its derivative decays exponentially $\dot{G}(t) \sim \exp(-\lambda t)$, where λ^{-1} is the longest relaxation time of the process ($\lambda = \Omega$ in the overdamped limit (5)). This leads to an exponential decay $p_{\text{TP}}(t) \sim \exp(-\lambda t)$ for the long time behavior of the distribution both in the overdamped and inertial case.¹⁸ In the next Section we compute $G(t)$ for a process with correlated and active noise and discuss the TPT distribution obtained from it.

Memory effects in transition path times

A reaction coordinate x is by definition a slow variable for which standard statistical mechanical arguments show that its time evolution is given in terms of a generalized Langevin equation.³⁰ For a parabolic barrier in the overdamped case this equation takes the form

$$\int_0^t K(t-\tau) \dot{x}(\tau) d\tau = kx(t) + \xi(t) \quad (6)$$

Here $K(t)$ is a memory kernel. The noise $\xi(t)$ is assumed to be a Gaussian process with average zero and a correlation that in equilibrium is related to $K(t)$ by the fluctuation-dissipation theorem

$$\langle \xi(t)\xi(t') \rangle = k_B T K(|t-t'|) \quad (7)$$

We focus here on a power law memory kernel

$$K(t) = \frac{\eta_\alpha t^{-\alpha}}{\Gamma(1-\alpha)} \quad (8)$$

where $0 < \alpha \leq 1$ and where, following Ref.,²⁷ we define the generalized friction coefficient as $\eta_\alpha = \gamma \Gamma(3-\alpha)$. In the limit $\alpha \rightarrow 1^-$, the Γ function in the denominator becomes singular and $K(t) = 2\gamma\delta(t)$, i.e. one recovers the Markovian (memoryless) dynamics. Power law kernels are found, for instance, in the dynamics of polymers which are characterized by a longest relaxation time τ_R . While on time scales much larger than τ_R the effects of memory on the motion of a reaction coordinate can be neglected, these are strongly influencing the polymer dynamics for $t < \tau_R$. Polymers have a memory kernel $K(t)$ that, for $t < \tau_R$, can be well approximated by a power law.^{31,32} This power law behavior is a characteristic of systems with a broad spectrum of relaxation times. **A priori, it is not clear which type of friction term $K(t)$ would adequately describe molecular folding experiments. We note that a power-law friction produces (for short times where the the effect of the force kx in Eq. (6) can be neglected) a mean square displacement growing as $\sim t^\alpha$. Subdiffusive behavior, corresponding to $\alpha < 1$, has been observed in simulations or experiments of protein dynamics, see eg.²⁰ and references therein. This suggests that a power-law kernel of the type (8) is a suitable candidate to model the dynamics of a one dimensional reaction coordinate in molecular folding.**

The generalized Langevin equation (6) with the kernel (8) is a linear equation which can be solved using Laplace transforms. The initial condition is $x(t=0) = -x_0$. As explained in the previous section we do not impose specific boundary conditions in $\pm x_0$, an approximation which is good for steep barriers $\beta E \gg 1$. The solution of (6) is (for details see Appendix)

$$x(t) = -x_0 \Theta_\alpha(t) + \frac{1}{\eta_\alpha} \int_0^t \xi(t-\tau) \Psi_\alpha(\tau) d\tau \quad (9)$$

where we introduced the functions

$$\Theta_\alpha(t) \equiv E_{\alpha,1}[(\Omega t)^\alpha] \quad (10)$$

$$\Psi_\alpha(t) \equiv t^{\alpha-1} E_{\alpha,\alpha}[(\Omega t)^\alpha] \quad (11)$$

($\Omega \equiv (k/\eta_\alpha)^{1/\alpha}$ is the characteristic rate of the process) and where

$$E_{\alpha,\beta}(z) \equiv \sum_{n=0}^{\infty} \frac{z^n}{\Gamma(\alpha n + \beta)} \quad (12)$$

is the Mittag-Leffler function.³³

We assume that the noise $\xi(t)$ is Gaussian, and since the Langevin equation (6) is linear, we conclude that also $x(t)$ is Gaussian. Hence Eqs. (1) and (2) apply. One has for the average

$$\bar{x}(t) \equiv \langle x(t) \rangle = -x_0 \Theta_\alpha(t) \quad (13)$$

while the variance is given by

$$\sigma^2(t) = \frac{k_B T}{k} (\Theta_\alpha^2(t) - 1) \quad (14)$$

(details of the calculations are in Appendix).

Plugging in (13) and (14) in (2) we get:

$$G(t) = \sqrt{\beta E} \sqrt{\frac{\Theta_\alpha(t) + 1}{\Theta_\alpha(t) - 1}} \quad (15)$$

This result generalizes the memoryless case (5), which is recovered in the limit $\alpha = 1$ since $\Theta_1(x) = E_{1,1}(x) = \exp(x)$.

Figure 1 shows plots of the transition path distribution $p_{\text{TP}}(t)$ for three different values of α and for two different values of k . The transition path time (in dimensionless units) decreases with decreasing α . We now look at the behavior of $p_{\text{TP}}(t)$ for small and large times which can be obtained from the corresponding behavior of the Mittag-Leffler functions. As the Mittag-Leffler functions diverge for diverging values of their arguments (15) implies that $G(t) \rightarrow \sqrt{\beta E}$ for $t \rightarrow \infty$. For $\dot{G}(t)$ one finds (for details see Appendix).

$$\dot{G}(t) \xrightarrow{t \rightarrow \infty} -e^{-\Omega t} \quad (16)$$

which implies that $p_{\text{TP}}(t)$ vanishes exponentially, as was the case for the Markovian **limit**

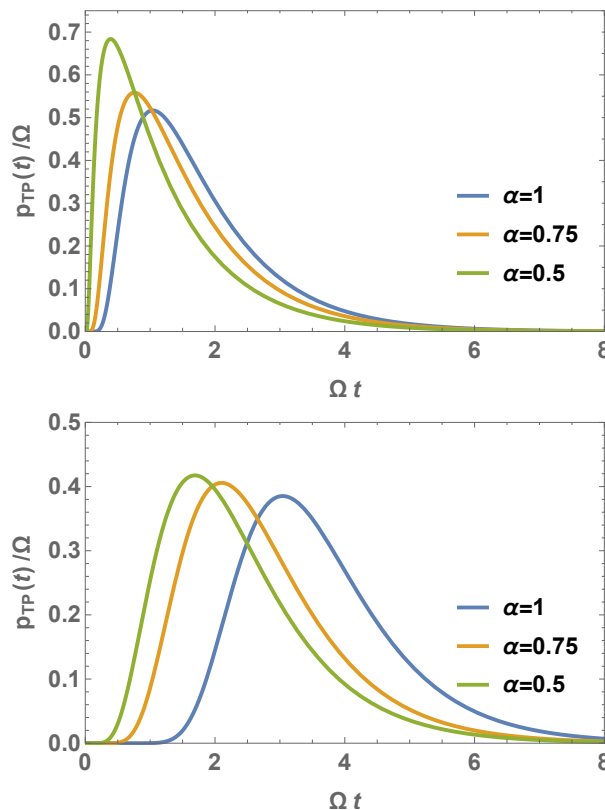


Figure 1: Transition path time distribution $p_{\text{TP}}(\Omega t)/\Omega$ for $\alpha = 1$ (blue), $\alpha = .75$ (orange) and $\alpha = 0.5$ (green). The other parameters are $k = 1$, $\eta_\alpha = 10$, $k_B T = 1$ and $x_0 = \sqrt{2}$ (top), $x_0 = \sqrt{20}$ (bottom), corresponding to $\beta E = 1$ and $\beta E = 10$, respectively.

$\alpha \rightarrow 1^-$.¹⁸ This is in contrast with the conclusions of a recent paper²⁰ where a stretched exponential decay was found. However, the results of that paper were obtained from a Fokker-planck equation for systems with memory that is only correct for a linear potential, or for small times.³⁴ Hence one cannot expect that it gives a correct asymptotic result.

For $t \rightarrow 0$, one has that $G^2(t) \rightarrow 2\beta E \Gamma(1 + \alpha)(\Omega t)^{-\alpha}$ (see (51)) from which it follows that $\dot{G}(t) \sim t^{-\alpha/2-1}$. The behavior of the transition path time distribution for early times is therefore determined by the essential singularity in $e^{-G^2(t)}$. Hence

$$p_{\text{TP}}(t) \xrightarrow{t \rightarrow 0} e^{-G^2(t)} \xrightarrow{t \rightarrow 0} \exp\left(-\frac{2\beta E \Gamma(1 + \alpha)}{(\Omega t)^\alpha}\right) \quad (17)$$

We see that the early time behavior does depend on α and that the exponent could be de-

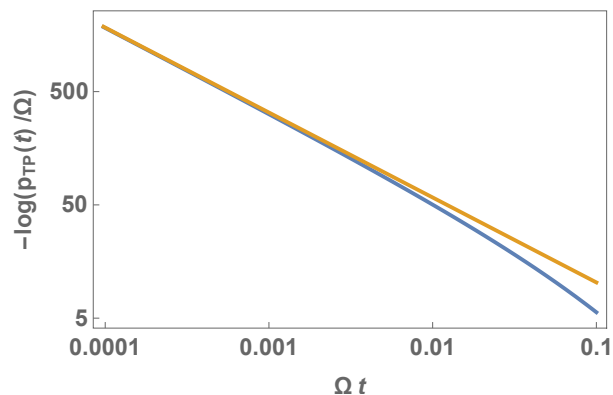


Figure 2: Log-log plot of $-\log(p_{TP}(t)/\Omega)$ versus Ωt for $\alpha = 0.75, k = 2, x_0 = 1$ in the early time regime $\Omega t < 0.1$. The blue line shows the exact expression while the orange line gives the early time approximation (17).

terminated from a straight line fit to a log-log plot of $-\log(p_{TP}(t)/\Omega)$ versus Ωt . In Fig. 2 we have made such a plot for $\alpha = 0.75$ and $\beta E = 1$. We find the expected power law behavior for $\Omega t < 0.005$. An integration of the TPT distribution shows however that the probability that the transition path time is in this regime is extremely low ($\sim 10^{-43}$). We therefore conclude that it is experimentally impossible to determine the exponent α from the early time behavior of the TPT.

We look next at the behavior of the average transition path time following the same procedure as outlined in Ref.¹⁸ As G is a monotonic decreasing function of t for the calculation it is convenient to perform a change of variable:

$$\langle t_{TP} \rangle = \int_0^\infty t p_{TP}(t) dt = \frac{\int_{\sqrt{\beta E}}^\infty t(G) e^{-G^2} dG}{\int_{\sqrt{\beta E}}^\infty e^{-G^2} dG} \quad (18)$$

The integral in the numerator can not be performed exactly. We can however get an approximation for βE sufficiently large. In that limit the integrals in (18) are determined by the large t -limit of $G(t)$. The average TPT is then given by (for details, see Appendix)

$$\langle t_{TP} \rangle = \frac{1}{\Omega} \log(2\alpha e^C \beta E) + \mathcal{O}\left(\frac{1}{\beta E}\right) \quad (19)$$

where $C \approx 0.577215$ is the Euler-Mascheroni

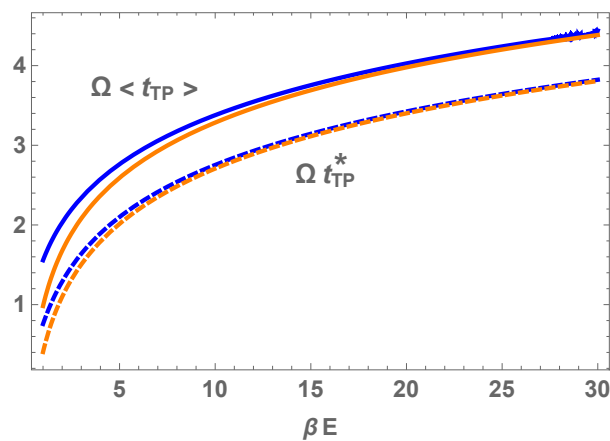


Figure 3: Average dimensionless transition path time, $\Omega \langle t_{TP} \rangle$ (solid lines), and most likely value Ωt_{TP}^* (dashed lines) as a function of the dimensionless energy βE for $\alpha = 0.75, k = 0.1, \eta_\alpha = 1$. The blue curves are obtained numerically from the exact expression for $p_{TP}(t)$, while the orange curves are the approximations (19) and (20).

constant (in the Markovian limit $\alpha = 1$ this expression coincides with that previously obtained by Szabo³⁵). In Fig. 3, we have plotted the result of a numerical calculation of the average transition path time as a function of βE using the full expression for $G(t)$ and compared it with the approximation (19) for $\alpha = .75$. We remark that, according to (19), the dimensionless average transition path time, $\Omega \langle t_{TP} \rangle$, decreases with decreasing α as was already evident from the plots in Fig. 1. The most likely transition path time t_{TP}^* , corresponding to the maximum of a distribution is (see Appendix)

$$t_{TP}^* = \frac{1}{\Omega} \log(2\alpha \beta E) + \mathcal{O}\left(\frac{1}{\beta E}\right) \quad (20)$$

and show a similar logarithmic dependence on the barrier height as the average (19). The comparison between the analytical expression (20) and the numerical calculation of the maximum is shown in Fig. 3 as dashed lines.

Transition path times in the presence of active forces

The folding of a biopolymer *in vivo* takes place in an environment which is out of equilibrium due to the action of various ATP-dependent active processes within a cell. These processes are known to modify the dynamics of various "probes" like microspheres³⁶⁻³⁸ and chromosomal loci.³⁹⁻⁴⁴ Typically, the active forces lead to an enhanced diffusion or even superdiffusive behavior. Similar phenomena have been observed in artificial acto-myosin networks.⁴⁵⁻⁴⁹ It has been found that the effect of the underlying motor processes can often be described in terms of an active noise $\eta(t)$ which is correlated over the time scale τ_A that the motors work. These times are of the order of seconds.

In a recent study on the behavior of active Brownian particles near soft walls, the dynamics of a semiflexible polymer immersed in an environment of such particles was investigated.⁵⁰ Active Brownian particles move in a direction \vec{e} which is subject to rotational Brownian diffusion. The force they produce on a (flexible) soft wall (like, for example a polymer) will therefore be exponentially correlated, where now the timescale τ_A of the correlation is related to the rotational diffusion constant. It was found that due to pressure instabilities, a sufficiently long polymer folds, even in the absence of interactions among the monomers.

Inspired by these two examples of folding in a non-equilibrium environment, it may be of interest to study also the effect of active forces on transition path times. We start from the Langevin equation

$$\gamma \dot{x}(t) = k x(t) + \xi(t) + \eta(t) \quad (21)$$

Here $\xi(t)$ is now a Markovian thermal force while $\eta(t)$ is the active noise which assume to have an exponential correlation.

$$\langle \eta(t) \eta(t') \rangle = C \exp \left(-\frac{|t - t'|}{\tau_A} \right) \quad (22)$$

We also take $\langle \eta(t) \rangle = 0$. The coefficient C measures the strength of the active force. There

is no associated friction force so that (21) describes a system out of equilibrium.

The solution of (21) with initial condition $x(t = 0) = -x_0$ is

$$x(t) = -x_0 e^{\Omega t} + \frac{1}{\gamma} \int_0^t e^{\Omega(t-t')} (\xi(t') + \eta(t')) dt'$$

From this we find that the deterministic motion is

$$\bar{x}(t) = \langle x(t) \rangle = -x_0 e^{\Omega t} \quad (23)$$

while the variance of the position is given by

$$\begin{aligned} \sigma^2(t) &= \langle (x(t) - \bar{x}(t))^2 \rangle \\ &= \left(\frac{k_B T}{k} + \frac{C \tau_A \Omega}{k^2 (1 - \tau_A \Omega)} \right) (e^{2\Omega t} - 1) \\ &\quad + \frac{2C \tau_A^2 \Omega^2}{k^2 (\tau_A^2 \Omega^2 - 1)} (e^{2\Omega t} - e^{(1-1/\Omega \tau_A)\Omega t}) \end{aligned} \quad (24)$$

It is convenient to describe the escape over the parabolic in terms of an effective temperature as was done in a study of the motion of colloids in active bath of bacteria and in the presence of a confining harmonic potential.⁵¹

Asymptotically $\sigma^2(t) e^{-2\Omega t}$ goes to a constant which can be used to define this effective temperature T^*

$$\begin{aligned} \lim_{t \rightarrow \infty} \sigma^2(t) e^{-2\Omega t} &= \frac{1}{k} \left[k_B T + \frac{C \tau_A \Omega}{k (\tau_A \Omega + 1)} \right] \\ &\equiv \frac{k_B T^*}{k} \end{aligned}$$

The effective temperature takes over the role of the physical temperature in the transition path time distribution. Going through the calculations of Ref.¹⁸ we find that in this case

$$p_{\text{TP}}(t) = -\frac{2}{\sqrt{\pi}} \frac{\dot{G}(t) e^{-G^2(t)}}{1 - \text{Erf}(\sqrt{\beta^* E})} \quad (25)$$

where $G(t)$ is given by (2) and $\beta^* = 1/k_B T^*$.

From these results one can find that at early times, the transition path time is again governed by the essential singularity in $e^{-G^2(t)}$ whose form is not modified by the active forces. The late time decay is governed by $\dot{G}(t)$ which

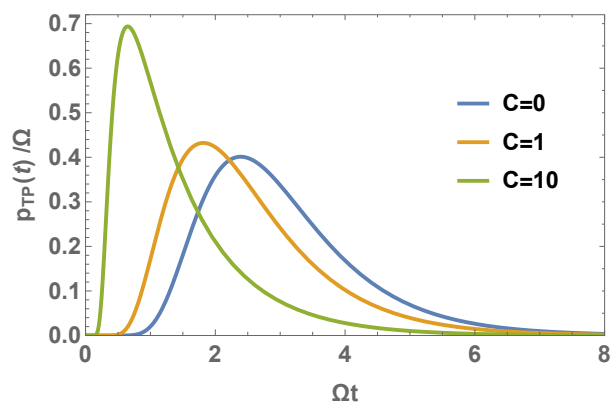


Figure 4: Transition path time distribution $p_{TP}(\Omega t)/\Omega$ for $C = 0$ (blue), $C = 1$ (orange) and $C = 10$ (green) and for $k = 0.1, \eta_\alpha = 1, x_0 = 10, k_B T = 1, \tau_A = 1$.

decays exponentially. The only change is in the prefactor of the exponential which now involves the effective temperature

$$\dot{G}(t) \sim -\sqrt{\beta^* E} \Omega e^{-\Omega t} \quad (t \rightarrow \infty) \quad (26)$$

Finally, in the expression for the average transition path time, the effective temperature also replaces the real temperature

$$\langle t_{TP}(t) \rangle = \Omega^{-1} \log(2e^C \beta^* E) \quad (27)$$

Since $\beta^* < \beta$, the addition of active forces leads to a decrease of the average transition path time. In Fig. 4, we have plotted some distributions where it can be seen that indeed the average transition path time decreases if the effective temperature (here tuned by changing C at fixed τ_A) increases.

As can be seen from the expression of the effective temperature, the dependence on τ_A is weak once it becomes bigger than Ω^{-1} (the other time scale in problem). This can also be seen in Fig. 5 where C is fixed and τ_A is increased from values below to values above Ω^{-1} .

Discussion

Conformational transitions of molecular systems between two different states are governed by two time scales. The Kramers time cor-

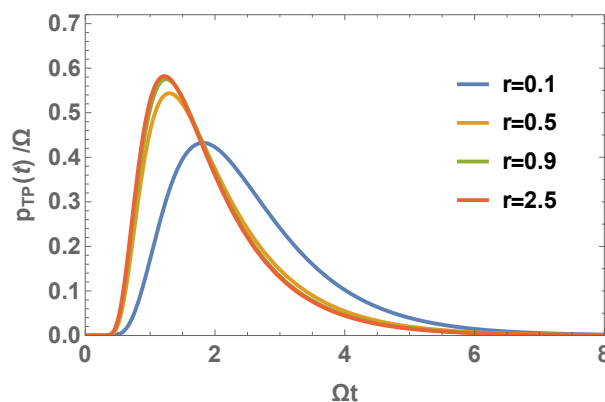


Figure 5: Transition path time distribution $p_{TP}(\Omega t)/\Omega$ for $r = 0.1$ (blue), $r = 0.5$ (orange) and $r = 0.9$ (green) and $r = 2.5$ (red) and for $k = 0.1, \eta_\alpha = 1, x_0 = 10, k_B T = 1, C = 1$. Here $r = \Omega \tau_A$ is the ratio of the two timescales in the problem.

responds to the typical time spent in a given conformation (the dwell time), while the transition path time characterizes the actual duration of the transition. Transition path times, which have been measured in proteins and nucleic acids folding experiments during the past decade,^{3-6,35} can be a few orders of magnitudes shorter than Kramers' times.

In this paper we have analyzed the TPT distribution of a one dimensional stochastic particle undergoing Langevin dynamics and crossing a parabolic barrier. We investigated the effects of memory and non-equilibrium thus extending previous analysis.^{10,18} As the barrier is parabolic, the associated Langevin equation is linear and hence exactly solvable in the case of free boundary conditions. This solution is expected to approximate very well the absorbing boundary case for steep barriers.

In Ref.¹⁹ the effect of memory on transition path times was also investigated. The TPT-distribution was derived for an arbitrary memory kernel starting from an Hamiltonian formulation in which the particle dynamics is coupled to a bath of harmonic oscillators.¹⁹ We expect that the expressions reported in¹⁹ will agree with our results in the case of overdamped dynamics with power-law memory in the limit of high barriers. Our result for the power law kernel has the advantage that it is simple and

of the same form as in the Markovian case. We expect it to be easier to compare with experiments.

Long time limit of transition path time distribution: why exponential decay?

We have found that the asymptotic decay of the transition path time distribution remains exponential for both cases investigated and therefore has a remarkable universal behavior. This contrasts with the conclusions of Ref.²⁰ In that work, which employed a Fokker-Planck equation with a time dependent diffusion constant $D(t) \sim t^{\alpha-1}$, it was argued that the large time decay of the TPT is stretched exponential. However, it was shown that for a particle in a harmonic potential the correct expression for $D(t)$ coincides with that used in²⁰ only for short times.³⁴ This suggests that the asymptotic stretched exponential behavior reported in²⁰ cannot be trusted. A diffusion constant $D(t) \sim t^{\alpha-1}$ was also derived for a particle under constant force.³⁴

To get some more insights about the differences in the effect of memory kernels in the constant force and the parabolic barrier case let us consider the following equation

$$\int_0^t K(t-\tau) \dot{x}(\tau) d\tau = f \quad (28)$$

which describes the average motion of particle driven by a constant force f in a medium characterized by the exponent α . Using Laplace transforms we find $x(t) - x(0) \sim t^\alpha$, with the normal drift $x(t) - x(0) \sim t$ recovered in the Markovian limit $\alpha \rightarrow 1$. This behavior can be deduced from an effective medium description

$$\Gamma_{\text{eff}}(t) \dot{x}(t) \sim f \quad (29)$$

where the effective friction $\Gamma_{\text{eff}}(t) \sim t^{-\alpha+1}$, as expected from the time integral of memory kernel, grows with time due to memory effects (the result is consistent with the Einstein relation for the diffusion constant discussed in³⁴). This indicates the velocity $\dot{x}(t) \sim ft^{\alpha-1}$ decreases

with time, hence, the anomalous drift. In the parabolic barrier there is, however, a crucial difference. The effective medium description would give

$$\Gamma_{\text{eff}}(t) \dot{x}(t) \sim kx(t) \quad (30)$$

with solution

$$x(t) = -x_0 \exp [-(\Omega t)^\alpha] \quad (31)$$

which is a stretched exponential behavior. This is not consistent with the exact solution of the generalized Langevin equation discussed in this paper, which yields for the average position an exponentially growing function at long times (obtained from the asymptotic behavior of the Mittag-Leffler function of (13)).

To understand this apparent paradox, we point out that the effective friction argument would be valid for a process in which the velocity $\dot{x}(t)$ is a slowly varying function. For a self-similar process, where the velocity changes according to a power law $\dot{x}(t) \sim t^{-\gamma}$, the coarse grained variable $\int_0^t dt' \dot{x}(t')/t \sim t^{-\gamma}$ by time average behaves similarly with the original variable. In such a case, the effective friction argument should work to get the correct scaling behavior.

However, in the parabolic barrier crossing, the velocity increases rapidly (exponentially), therefore, the contribution from the memory kernel integral is dominated by the most recent term only. This implies that in the long time scale, we should expect an effective description, in which the system feels only the instantaneous response, hence our effective equation is

$$\tilde{\gamma} \dot{x}(t) = kx(t) \quad (32)$$

where $\tilde{\gamma}$ is a renormalized friction coefficient. Our argument suggests that it is this renormalization that is behind the universal exponential decay in the long time limit of transition path time distribution. This asymptotic behavior sets already in at $\Omega t \simeq 1.5$ as seen numerically (Fig. 1).

Comparison with experiments: possible implications

Differently from the Kramers' time, which is characterised by an exponential dependence on the barrier height E , the average TPT in the overdamped limit scales logarithmically $\langle t_{\text{TP}} \rangle \sim \log(\beta E)$, where β is the inverse temperature. We have shown here that the logarithmic dependence also holds in the presence of memory effects or of active forces. The effect of the active forces is simply to increase the temperature to a higher effective one. Hence the average TPT will always decrease in this case. Memory also decrease the average TPT when measured in dimensionless units.

One of the currently puzzling aspects of TPT experiments is the inconsistency of values of the barrier height estimated from different methods.⁷ More precisely, the analysis of the TPT distribution yields values for βE that are more than one order of magnitude lower than those determined from the analysis of Kramers' folding times.⁷ While some explanations of this discrepancies have been recently proposed,^{19,20} we point out here that both memory (as also discussed in²⁰) and for noise of non-thermal origin lead to an effective lowering of the potential barrier, by decreasing the TPT. Further research will have to show whether this qualitative agreement can be made more quantitative.

Acknowledgement Discussions with M. Caraglio and M. Laleman are gratefully acknowledged.

Appendix A: Power law memory kernel

The solution of the generalized Langevin equation (6) with power law memory kernel is obtained by performing its Laplace transform

$$\tilde{K}(s) (s\tilde{x}(s) + x_0) = k\tilde{x}(s) + \tilde{\xi}(s) \quad (33)$$

where $\tilde{f}(s)$ indicates the Laplace transform of the function $f(t)$. To obtain the previous equation we used the convolution theorem (the

Laplace transform of a convolution product is the product of the Laplace transforms) and the fact that the Laplace transform of a derivative is

$$\tilde{\dot{f}} = s\tilde{f}(s) - f(0) \quad (34)$$

(in our case the initial condition is $x(0) = -x_0$). Solving (33) we get

$$\tilde{x}(s) = \frac{-x_0\tilde{K}(s)}{s\tilde{K}(s) - k} + \frac{\tilde{\xi}(s)}{s\tilde{K}(s) - k} \quad (35)$$

The Laplace transform of the power law kernel (8) is

$$\tilde{K}(s) = \gamma s^{\alpha-1} \quad (36)$$

therefore Eq. (35) takes the form

$$\tilde{x}(s) = \frac{-x_0 s^\alpha}{s(s^\alpha - k/\gamma)} + \frac{1}{\gamma} \frac{\tilde{\xi}(s)}{s^\alpha - k/\gamma} \quad (37)$$

To perform the inverse transform we use the following relation

$$\int_0^\infty dt e^{-ts} t^{\beta-1} E_{\alpha,\beta}(at^\alpha) = \frac{s^\alpha}{s^\beta(s^\alpha - a)} \quad (38)$$

where $E_{\alpha,\beta}(z)$ is known as Mittag-Leffler function.³³ To handle the two terms in the left hand side of (37) one can use (38) with $\beta = 1$ and $\beta = \alpha$. For this purpose it is convenient to introduce the functions

$$\Theta_\alpha(t) \equiv E_{\alpha,1}[(\Omega t)^\alpha] \quad (39)$$

$$\Psi_\alpha(t) \equiv t^{\alpha-1} E_{\alpha,\alpha}[(\Omega t)^\alpha] \quad (40)$$

where $\Omega \equiv (k/\gamma)^{1/\alpha}$ is a characteristic rate of the process. Inverting (37) we get

$$x(t) = -x_0\Theta_\alpha(t) + \frac{1}{\gamma} \int_0^t \xi(t-\tau)\Psi_\alpha(\tau)d\tau \quad (41)$$

Averaging over noise we get the average position, or equivalently the deterministic solution

$$\bar{x}(t) = -x_0\Theta_\alpha(t) \quad (42)$$

while the variance (4) is

$$\begin{aligned}\sigma^2(t) &= \frac{k_B T}{\gamma} \int_0^t d\tau d\sigma \frac{|\tau - \sigma|^{-\alpha}}{\Gamma(1-\alpha)} \Psi_\alpha(\tau) \Psi_\alpha(\sigma) \\ &= \frac{k_B T}{k} (\Theta_\alpha^2(t) - 1)\end{aligned}\quad (43)$$

(the details of the calculation of this integral are given in Appendix). We finally combine the above results to find $G(t)$, see (2)

$$G(t) = \frac{x_0 - \bar{x}(t)}{\sqrt{2\sigma^2(t)}} = \sqrt{\beta E} \sqrt{\frac{\Theta_\alpha(t) + 1}{\Theta_\alpha(t) - 1}} \quad (44)$$

where $E = kx_0^2/2$ is the barrier height. This proves Eq. (15) of the main text.

The Mittag-Leffler function behaves asymptotically as³³

$$E_{\alpha,\beta}(z) \xrightarrow{z \rightarrow \infty} \frac{1}{\alpha} z^{(1-\beta)/\alpha} \exp(z^{1/\alpha}) \quad (45)$$

which implies

$$\Theta_\alpha(t) \xrightarrow{t \rightarrow \infty} \frac{1}{\alpha} \exp(\Omega t) \quad (46)$$

Hence

$$G(t) \xrightarrow{t \rightarrow \infty} \sqrt{\beta E} \quad (47)$$

$$\dot{G}(t) \xrightarrow{t \rightarrow \infty} -\sqrt{\beta E} \alpha \Omega \exp(-\Omega t) \quad (48)$$

For small arguments, the Mittag-Leffler function behaves as³³

$$E_{\alpha,\beta}(z) = 1 + \frac{z^\alpha}{\Gamma(\alpha + \beta)} + \dots \quad (49)$$

hence

$$\Theta_\alpha(t) = 1 + \frac{(\Omega t)^\alpha}{\Gamma(1 + \alpha)} + \dots \quad (50)$$

This implies that $G(t)$ diverges for small t

$$G(t) \sim (\Omega t)^{-\alpha/2} \quad (51)$$

The average transition path time

To calculate the average TPT we follow the calculation outlined in:¹⁸

$$\langle t_{TP} \rangle = \int_0^\infty t p_{TP}(t) dt = \frac{\int_{\sqrt{\beta E}}^\infty t(G) e^{-G^2} dG}{\int_{\sqrt{\beta E}}^\infty e^{-G^2} dG} \quad (52)$$

where we have made the change of variables $G' dt = dG$ and used the definition of the error function. The integral in the numerator can not be performed exactly. We can get an approximation for $\beta E \gg 1$ where the integrals are determined by the large t -limit of $G(t)$. From (39), (44) and (45) one gets for t large

$$G(t) = \sqrt{\beta E} [1 + \alpha e^{-\Omega t} + \dots] \quad (53)$$

which can be inverted to

$$t = \frac{1}{\Omega} \left(\log \alpha - \log \left(\frac{G}{\sqrt{\beta E}} - 1 \right) \right) \quad (54)$$

If we insert (54) into (52) and make also here an expansion for large βE we finally get

$$\langle t_{TP} \rangle = \frac{1}{\Omega} \log(2\alpha e^C \beta E) + O\left(\frac{1}{\beta E}\right) \quad (55)$$

where $C \approx 0.577215$ is the Euler-Mascheroni constant.

The most likely transition path time

Another interesting quantity we can infer from the results is t_{TP}^* , the most likely value of the TPT. This is obtained by solving the equation

$$\frac{dp_{TP}}{dt} = 0 \quad (56)$$

which from (1) implies $\ddot{G} = 2G\dot{G}^2$ (where the dot indicates the time derivative), or using (15):

$$\dot{\Theta}_\alpha^2 - \ddot{\Theta}_\alpha (\Theta_\alpha^2 - 1) + 2\Theta_\alpha \dot{\Theta}_\alpha^2 = 2\beta E \dot{\Theta}_\alpha^2 \frac{\Theta_\alpha + 1}{\Theta_\alpha - 1} \quad (57)$$

Using the asymptotic $t \rightarrow +\infty$ expansion (46) one has

$$\dot{\Theta}_\alpha(t) \sim \frac{\Omega}{\alpha} \exp(\Omega t), \quad \ddot{\Theta}_\alpha(t) \sim \frac{\Omega^2}{\alpha} \exp(\Omega t) \quad (58)$$

and to leading order in βE the solution of (57) becomes

$$t_{\text{TP}}^* = \frac{1}{\Omega} \log(2\alpha\beta E) \quad (59)$$

Appendix B: Integral (43)

To compute the integral (43) we start from the double Laplace transform of the function $\Theta_\alpha(|\tau - \sigma|)$. We have

$$f(s, s') \equiv \int_0^{+\infty} \int_0^{+\infty} d\tau d\sigma e^{-s\tau - s'\sigma} \Theta_\alpha(|\tau - \sigma|) \quad (60)$$

To get rid of the absolute value we split the integral in two domains so to obtain

$$\begin{aligned} f(s, s') &= \int_0^{+\infty} d\tau \int_\tau^{+\infty} d\sigma e^{-s\tau - s'\sigma} \Theta_\alpha(\sigma - \tau) \\ &+ \int_0^{+\infty} d\sigma \int_\sigma^{+\infty} d\tau e^{-s\tau - s'\sigma} \Theta_\alpha(\tau - \sigma) \\ &= \frac{1}{s + s'} \left[\frac{1}{s'(1 - (\Omega/s')^\alpha)} + \frac{1}{s(1 - (\Omega/s)^\alpha)} \right] \end{aligned} \quad (61)$$

The integrals can be easily computed using a change of variables and the property (38). The above expression can be rearranged as follows

$$f(s, s') = \frac{1}{s s' (1 - (\Omega/s')^\alpha) (1 - (\Omega/s)^\alpha)} - \frac{\Omega^\alpha}{(s s')^\alpha (1 - (\Omega/s')^\alpha) (1 - (\Omega/s)^\alpha)} \frac{s^{\alpha-1} + s'^{\alpha-1}}{s + s'} \quad (62)$$

The double inverse Laplace transform of the first term is easy as this term is the product of a function of s and a function of s' . One has two independent inverse Laplace transform and from (38) one sees that this generates $\Theta_\alpha(\tau)\Theta_\alpha(\sigma)$.

The second term in (62) is a product of two fractions. In the first one, one recognises the

double Laplace transform of $\Omega^\alpha \Psi_\alpha(\tau)\Psi_\alpha(\sigma)$. For the second one we use

$$\int_0^{+\infty} d\tau d\sigma \frac{e^{-\sigma s - \tau s'} |\tau - \sigma|^{-\alpha}}{\Gamma(1 - \alpha)} = \frac{s^{\alpha-1} + s'^{\alpha-1}}{s + s'} \quad (63)$$

Invoking the convolution theorem of double Laplace transforms, the second term of (62) is therefore the double Laplace transform of the convolution

$$\frac{\Omega^\alpha}{\Gamma(1 - \alpha)} \int_0^t \int_0^{t'} d\tau d\sigma |\tau - \sigma|^{-\alpha} \Psi_\alpha(\tau) \Psi_\alpha(\sigma) \quad (64)$$

Putting everything together we have

$$\begin{aligned} \frac{\Omega^\alpha}{\Gamma(1 - \alpha)} \int_0^t \int_0^{t'} d\tau d\sigma |\tau - \sigma|^{-\alpha} \Psi_\alpha(\tau) \Psi_\alpha(\sigma) \\ = \Theta_\alpha(t)\Theta_\alpha(t') - \Theta_\alpha(|t - t'|) \end{aligned} \quad (65)$$

from which (43) follows by putting $t = t'$.

References

- (1) Hänggi, P.; Talkner, P.; Borkovec, M. Reaction-rate theory: fifty years after Kramers. *Rev. Mod. Phys.* **1990**, *62*, 251.
- (2) Hummer, G. From transition paths to transition states and rate coefficients. *J. Chem. Phys.* **2004**, *120*, 516–523.
- (3) Chung, H. S.; Louis, J. M.; Eaton, W. A. Experimental determination of upper bound for transition path times in protein folding from single-molecule photon-by-photon trajectories. *Proc. Natl. Acad. Sci. USA* **2009**, *106*, 11837–11844.
- (4) Neupane, K.; Ritchie, D. B.; Yu, H.; Foster, D. A. N.; Wang, F.; Woodside, M. T. Transition path times for nucleic Acid folding determined from energy-landscape analysis of single-molecule trajectories. *Phys. Rev. Lett.* **2012**, *109*, 068102.
- (5) Truex, K.; Chung, H. S.; Louis, J. M.; Eaton, W. A. Testing landscape the-

- ory for biomolecular processes with single molecule fluorescence spectroscopy. *Phys. Rev. Lett.* **2015**, *115*, 018101.
- (6) Neupane, K.; Wang, F.; Woodside, M. T. Direct measurement of sequence-dependent transition path times and conformational diffusion in DNA duplex formation. *Proc. Natl. Acad. Sci. USA* **2017**, 201611602.
- (7) Neupane, K.; Foster, D. A.; Dee, D. R.; Yu, H.; Wang, F.; Woodside, M. T. Direct observation of transition paths during the folding of proteins and nucleic acids. *Science* **2016**, *352*, 239–242.
- (8) Berezhkovskii, A.; Szabo, A. One-dimensional reaction coordinates for diffusive activated rate processes in many dimensions. *J. Chem. Phys.* **2005**, *122*, 014503.
- (9) Dudko, O. K.; Hummer, G.; Szabo, A. Intrinsic rates and activation free energies from single-molecule pulling experiments. *Phys. Rev. Lett.* **2006**, *96*, 108101.
- (10) Zhang, B. W.; Jasnow, D.; Zuckerman, D. M. Transition-event durations in one-dimensional activated processes. *J. Chem. Phys.* **2007**, *126*, 074504.
- (11) Sega, M.; Faccioli, P.; Pederiva, F.; Garberoglio, G.; Orland, H. Quantitative protein dynamics from dominant folding pathways. *Phys. Rev. Lett.* **2007**, *99*, 118102.
- (12) Chaudhury, S.; Makarov, D. E. A harmonic transition state approximation for the duration of reactive events in complex molecular rearrangements. *J. Chem. Phys.* **2010**, *133*, 034118.
- (13) Orland, H. Generating transition paths by Langevin bridges. *J. Chem. Phys.* **2011**, *134*, 174114.
- (14) Kim, W. K.; Netz, R. R. The mean shape of transition and first-passage paths. *J. Chem. Phys.* **2015**, *143*, 224108.
- (15) Makarov, D. E. Shapes of dominant transition paths from single-molecule force spectroscopy. *J. Chem. Phys.* **2015**, *143*, 194103.
- (16) Daldrop, J. O.; Kim, W. K.; Netz, R. R. Transition paths are hot. *EPL (Europhysics Letters)* **2016**, *113*, 18004.
- (17) Berezhkovskii, A. M.; Dagdug, L.; Bezrukov, S. M. Mean Direct-Transit and Looping Times as Functions of the Potential Shape. *J. Phys. Chem. B* **2017**, *121*, 5455.
- (18) Laleman, M.; Carlon, E.; Orland, H. Transition path time distributions. *J. Chem. Phys.* **2017**, *147*, 214103.
- (19) Pollak, E. Transition path time distribution and the transition path free energy barrier. *Phys. Chem. Chem. Phys.* **2016**, *18*, 28872.
- (20) Satija, R.; Das, A.; Makarov, D. E. Transition path times reveal memory effects and anomalous diffusion in the dynamics of protein folding. *J. Chem. Phys.* **2017**, *147*, 152707.
- (21) Sakaue, T. Nonequilibrium dynamics of polymer translocation and straightening. *Phys. Rev. E* **2007**, *76*, 021803.
- (22) Panja, D.; Barkema, G. T.; Ball, R. C. Anomalous dynamics of unbiased polymer translocation through a narrow pore. *Journal of Physics: Condensed Matter* **2007**, *19*, 432202.
- (23) Dubbeldam, J. L.; Rostiashvili, V.; Milchev, A.; Vilgis, T. A. Fractional Brownian motion approach to polymer translocation: The governing equation of motion. *Phys. Rev. E* **2011**, *83*, 011802.
- (24) Walter, J.-C.; Ferrantini, A.; Carlon, E.; Vanderzande, C. Fractional Brownian motion and the critical dynamics of zipping polymers. *Phys. Rev. E* **2012**, *85*, 031120.

- (25) Frederickx, R.; In't Veld, T.; Carlon, E. Anomalous dynamics of DNA hairpin folding. *Phys. Rev. Lett.* **2014**, *112*, 198102.
- (26) Sakaue, T.; Walter, J.-C.; Carlon, E.; Vanderzande, C. Non-Markovian dynamics of reaction coordinate in polymer folding. *Soft Matter* **2017**, *13*, 3174–3181.
- (27) Vandebroek, H.; Vanderzande, C. The effect of active fluctuations on the dynamics of particles, motors and DNA-hairpins. *Soft Matter* **2017**, *13*, 2181–2191.
- (28) Bechinger, C.; Di Leonardo, R.; Löwen, H.; Reichhardt, C.; Volpe, G.; Volpe, G. Active particles in complex and crowded environments. *Rev. Mod. Phys.* **2016**, *88*, 045006.
- (29) Caraglio, M.; Put, S.; Carlon, E.; Vanderzande, C. The influence of absorbing boundary conditions on the transition path times statistics. *arXiv preprint arXiv:1807.03011* **2018**,
- (30) Zwanzig, R. *Nonequilibrium Statistical Mechanics*; Oxford University Press, 2001.
- (31) Panja, D. Generalized Langevin equation formulation for anomalous polymer dynamics. *J. Stat. Mech.: Theory and Experiment* **2010**, *2010*, L02001.
- (32) Saito, T.; Sakaue, T. Driven anomalous diffusion: An example from polymer stretching. *Phys. Rev. E* **2015**, *92*, 012601.
- (33) Haubold, H. J.; Mathai, A. M.; Saxena, R. K. Mittag-Leffler functions and their applications. *Journal of Applied Mathematics* **2011**, *2011*.
- (34) Goychuk, I. Viscoelastic subdiffusion: Generalized Langevin equation approach. *Adv. Chem. Phys.* **2012**, *150*, 187.
- (35) Chung, H. S.; McHale, K.; Louis, J. M.; Eaton, W. A. Single-Molecule Fluorescence Experiments Determine Protein Folding Transition Path Times. *Science* **2012**, *335*, 981.
- (36) Caspi, A.; Granek, R.; Elbaum, M. Enhanced diffusion in active intracellular transport. *Phys. Rev. Lett.* **2000**, *85*, 5655.
- (37) Gal, N.; Weihs, D. Intracellular mechanics and activity of breast cancer cells correlate with metastatic potential. *Cell Biochem. Biophys.* **2012**, *63*, 199.
- (38) Goldstein, D.; Elhanan, T.; Aronovitch, M.; Weihs, D. Origin of active transport in breast-cancer cells. *Soft Matter* **2013**, *9*, 7167.
- (39) Weber, S.; Spakowitz, A.; Theriot, J. Non-thermal ATP-dependent fluctuations contribute to the in vivo motion of chromosomal loci. *Proc. Natl. Acad. Sci. USA* **2012**, *109*, 7338.
- (40) Javer, A.; Long, Z.; Nugent, E.; Grisi, M.; Siriawetchakul, K.; Dorfman, K.; Cicuta, P.; Cosentino Lagomarsino, M. Short-time movement of E. coli chromosomal loci depends on coordinate and sub-cellular localization. *Nat. Commun.* **2013**, *4*, 3003.
- (41) Javer, A.; Kuwada, N.; Long, Z.; Benza, V.; Dorfman, K.; Wiggins, P.; Cicuta, P.; Cosentino Lagomarsino, M. Persistent super-diffusive motion of Escherichia coli chromosomal loci. *Nat. Commun.* **2014**, *5*, 3854.
- (42) Zidovska, A.; Weitz, D.; Mitchinson, T. Micron-scale coherence in interphase chromatin dynamics. *Proc. Natl. Acad. Sci. USA* **2013**, *110*, 15555.
- (43) Sakaue, T.; Saito, T. Active diffusion of model chromosomal loci driven by athermal noise. *Soft Matter* **2017**, *13*, 81.
- (44) Arai, R.; Sugawara, T.; Sato, Y.; Minakuchi, Y.; Toyoda, A.; Nabeshima, K.; Kimura, H.; Kimura, A. Reduction in

chromosome mobility accompanies nuclear organization during early embryogenesis in *Caenorhabditis elegans*. *Scientific Reports* **2017**, *7*, 3631.

- (45) Soares e Silva, M.; Stuhmann, B.; Betz, T.; Koenderink, G. Time-resolved microrheology of actively remodeling actomyosin networks. *New J. Phys.* **2014**, *16*, 075010.
- (46) Stuhmann, B.; Soares e Silva, M.; Depken, M.; MacKintosh, F.; Koenderink, G. Nonequilibrium fluctuations of a remodeling in vitro cytoskeleton. *Phys. Rev. E* **2012**, *86*, 020901(R).
- (47) Toyota, T.; Head, D.; Schmidt, C.; Mizuno, D. Non-Gaussian athermal fluctuations in active gels. *Soft Matter* **2011**, *7*, 3234.
- (48) Brangwynne, C.; Koenderink, G.; MacKintosh, F.; Weitz, D. Nonequilibrium microtubule fluctuations in a model cytoskeleton. *Phys. Rev. Lett.* **2008**, *100*, 118104.
- (49) Fakhri, N.; Wessel, A.; Willms, C.; Pasquali, M.; Klopffensstein, D.; MacKintosh, F.; Schmidt, C. High-resolution mapping of intracellular fluctuations using carbon nanotubes. *Science* **2014**, *344*, 1031.
- (50) Nikola, N.; Solon, A. P.; Kafri, Y.; Kardar, M.; Tailleur, J.; Voituriez, R. Active particles with soft and curved walls: equation of state, ratchets and instabilities. *Phys. Rev. Lett.* **2016**, *117*, 098001.
- (51) Maggi, C.; Paoluzzi, M.; Pellicciotta, N.; Lepore, A.; Angelani, L.; Di Leonardo, R. Generalized energy equipartition in harmonic oscillators driven by active baths. *Phys. Rev. Lett.* **2014**, *113*, 238303.

Probability Distribution

